Waveform Tomography strategies for imaging attenuation structure with cross-hole data

Rie Kamei, R. Gerhard Pratt

Department of Geological Sciences and Engineering, Queen's University

Submitted to 70th EAGE Conference & Exhibition incorporating SPE EUROPEC 2008 on 20th January, 2008

SUMMARY

Waveform Tomography, when implemented in the frequency-domain, potentially yields images of the instrinsic attenuation from seismic waveform data. The attenuation (or its inverse, the seismic *Q* value) is strongly related to useful geological variables such as rheology, fluid flow, pore fluid content and fractures. Since phase and amplitude anomalies in recorded data are also caused by velocity structure (due to geometrical and scattering effects), it is critical to assess inversion strategies as to their ability to resolve these effects. In this study, frequency domain Waveform Tomography was implemented with the subspace-search method, and evaluated with synthetic tests. We compared two sets of strategies: first, velocity and attenuation models were updated jointly at each iteration ("simultaneous inversion"). In a second test, ("sequential inversion"), a velocity model alone was first inverted followed by simultaneous inversion. While the predicted waveforms from both strategies agreed with the observed data, only the sequential inversion strategy imaged attenuation structure well in the presence of small-scale velocity heterogeneities. This highlights the strong dependence of attenuation imaging on the quality of the velocity model.

MAIN OBJECTIVES

To evaluate Waveform Tomography strategies for imaging seismic attenuation structure. Synthetic benchmark data from a realistic crosshole environment were used to assess several approaches based on the sub-space search method, and a reliable methodology was developed that provided stable attenuation images in the presence of small scale scattering and complex velocity structures.

NEW ASPECTS COVERED

The imaging of seismic attenuation with Waveform Tomography is a new, and potentially fruitful area of study. Seismic attenuation is related to critical reservoir properties. In order to image these properties with confidence, we carried out a rigorous assessment of the methodology using benchmark synthetic data.

Introduction

Seismic Waveform Tomography is a multi-parameter problem: observed waveforms contain information not only on velocity structures, but also on various other parameters. Among these parameters, the attenuation (or its inverse, the seismic *Q* value) is strongly related to useful geological variables such as rheology, fluid flow, pore fluid content and fractures. The attenuation of seismic waveforms is caused by two mechanisms; absorption of energy due to rock properties (intrinsic *Q*), and scattering of energy corresponding to small-scale velocity fluctuation (scattering *Q*). Since the intrinsic *Q* is of primary interest in oil/gas exploration, it is desirable to separate the effects of scattering from the *Q* image. In heterogeneous media, seismic waveforms exhibit amplitude and phase anomalies due to *Q* structure. However, anomalies are also caused by velocity structure (due to geometrical and scattering effects), and it is critical to separate the effects of velocity from those of the attenuation parameters. Thus, to image both velocity and (intrinsic) attenuation structures accurately, we need an inversion scheme that 1) is high resolution in velocity to eliminate scattering effects, 2) handles defocussing/focussing effects properly, and 3) has good resolution between the velocity and *Q* parameters. In this work, we investigate Waveform Tomography methodologies for cross-hole surveys, in the presence of strong velocity and attenuation heterogeneities.

Method

Viscoacoustic Frequency-domain Waveform Tomography (Pratt et al., 1998, Hicks and Pratt, 2001, Pratt et al., 2004) may be used to image velocity and attenuation structures simultaneously. In contrast to ray-based inversions of first arrival times and/or amplitudes, Waveform Tomography incorporates non-linear scattered, refracted and reflected waves, and consequently achieves more accurate and better resolved images. Under the assumption that *Q* is large and frequency independent, intrinsic attenuation may be included in the acoustic wave equation by using a frequency-dependent complex-valued velocity,

$$c(\omega) = c_R(\omega) + ic_I(\omega)$$

where ω is an angular frequency, c_R is a phase velocity, and

$$Q = -c_R(\omega)/2c_I(\omega).$$

In the heterogeneous media we considered, both parameters are also assumed to vary with position. We incorporated the (intrinsic) *Q* - dispersion relationship of Liu et al. (1978) to satisfy causality. The full parameter set is denoted as

$$\mathbf{m} = \begin{bmatrix}\mathbf{m}^{(1)} & \mathbf{m}^{(2)}\end{bmatrix}^T$$

where $\mathbf{m}^{(1)}$ represents a velocity model, parameterised using the real part of the slowness (after Sirgue, 2003), and $\mathbf{m}^{(2)}$ is an attenuation model parameterised by the imaginary part of the slowness.

The subspace method (Kennet et al., 1988) was employed as an optimization algorithm. This allowed us to handle both velocity and attenuation parameters explicitly. In our implementation we optimized a model in a subspace consisting of two steepest descent directions (one for each parameter type). The model update direction is given by

$$\delta\mathbf{m} = \mathbf{A}(\mathbf{A}^T\mathbf{H}\mathbf{A})^{-1}\mathbf{A}^T\boldsymbol{\gamma} = \begin{bmatrix}\alpha^{(1)}\boldsymbol{\gamma}^{(1)T} & \alpha^{(2)}\boldsymbol{\gamma}^{(2)T}\end{bmatrix}^T$$

where $\boldsymbol{\gamma}$ is a steepest descent direction, $\mathbf{A} = \begin{bmatrix}\boldsymbol{\gamma}^{(1)} & \mathbf{0} \\ \mathbf{0} & \boldsymbol{\gamma}^{(2)}\end{bmatrix}$ is a projection matrix from the model space to the model subspace, $\boldsymbol{\gamma}^{(i)}$ is a steepest descent direction corresponding to $\mathbf{m}^{(i)}$, and $\alpha^{(i)}$ is a steplength to $\mathbf{m}^{(i)}$.

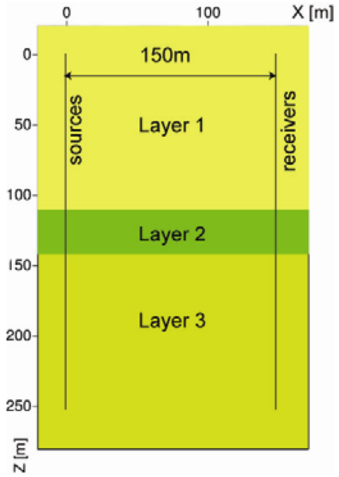

Figure 1: Schematic model. There are 125 sources and receivers with 2 m interval.

Inversions of synthetic waveforms

We created a three-layer model consisting of two lithology types with a cross-well survey geometry (Figures 1 and 2). The layers have the following characteristics: 1) In the top layer only one lithology is present and scattering attenuation is dominant – there are strong, small-scale velocity fluctuations and weak intrinsic attenuation. 2) The middle layer is a mixture of two distinct lithologies, one of them having strong intrinsic attenuation. 3) The bottom layer comprises a single lithology with small velocity heterogeneities and weak intrinsic attenuation. The synthetic velocity and attenuation models were deliberately left uncorrelated to allow the parameter resolution of the inversion approaches to be evaluated.

Synthetic acoustic waveforms were computed using a frequency domain finite difference code (Figure 3(a) and black lines in (c)-(e)). Waveforms in layer 1 and layer 2 show large amplitude losses around the first arrivals. Also in Layer1, each receiver recorded several arrivals of similar magnitudes in amplitudes.

We compared two sets of inversion strategies: first, velocity and attenuation models were updated jointly at each iteration ("simultaneous inversion"). In a second test, ("sequential inversion"), a velocity model was first inverted while fixing the starting 1/*Q* values, followed by simultaneous inversion. We started the inversions from a smoothed version of the true velocity model and a homogeneous *1/Q* model. Frequencies ranging from 100-850 Hz were used. Figure 3 shows the inverted models after simultaneous inversion alone, and the results of sequential inversion are presented in Figure 4.

Discussion and conclusions

The simultaneous inversion strategy was successful in resolving the velocity model (Figures 4(a)), but the estimated *1/Q* model showed strong and unreasonable fluctuation in layer 1 and layer 2 (Figures 4(b)). Nevertheless, the predicted waveforms after simultaneous inversion matched the observed data around the first arrivals, indicating the convergence of the inversion. When the sequential inversion strategy was used, the estimated velocity model showed higher wavenumber components, most of which were recovered during the initial velocity inversion (Figures 5(a)). The final 1/*Q* model was then much smoother, and the image resolved the two distinct lithologies in layer 2 very well (Figure 5(b)). The final predicted waveforms agree with the observed data for the entire record (Figure 3(b)-(e)).

We conclude from these results that attenuation Waveform Tomography is non-linear, and more strongly influenced by the quality of the starting velocity model than is velocity inversion alone. Thus an initial high-resolution velocity inversion should be performed prior to attempting to obtain a stable *Q* image. This is because the amplitude sensitivity to velocity structure is of the same magnitude as the sensitivity to intrinsic *Q* structure. Indeed, focussing/defocussing and scattering effects can create significant amplitude anomalies especially in relatively small-scale velocity fluctuations (e.g. layer 1, see Figure 3(c)). Due to the resolution limit predicted within the Born approximation (Wu and Toksoz, 1987), it is difficult to recover velocity fluctuations higher in wavenumber than $2k_o = 2/\lambda$. Without an accurate velocity model, the inversion compensates for observed amplitude anomalies by yielding an unstable 1/*Q* image. Note that because of limited bandwidth and data noise, it may be impossible to obtain a sufficiently high wavenumber velocity model under some conditions. We may therefore need appropriate regularization methods to stabilise the attenuation images when these are obtained from low-resolution velocity images.

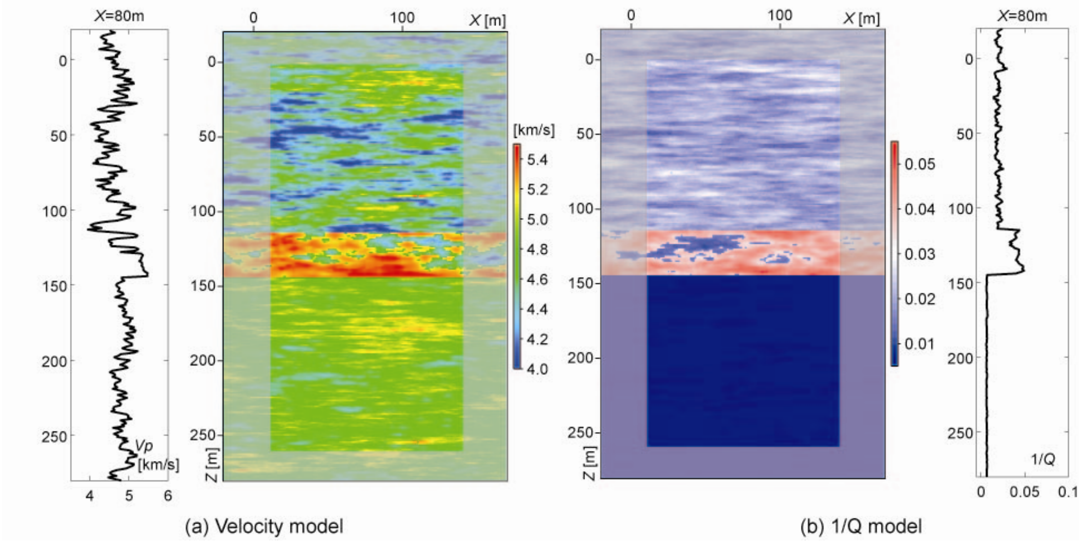

Figure 2: (a) True velocity model (b) true *1/Q* model with vertical profiles at *X*=80m

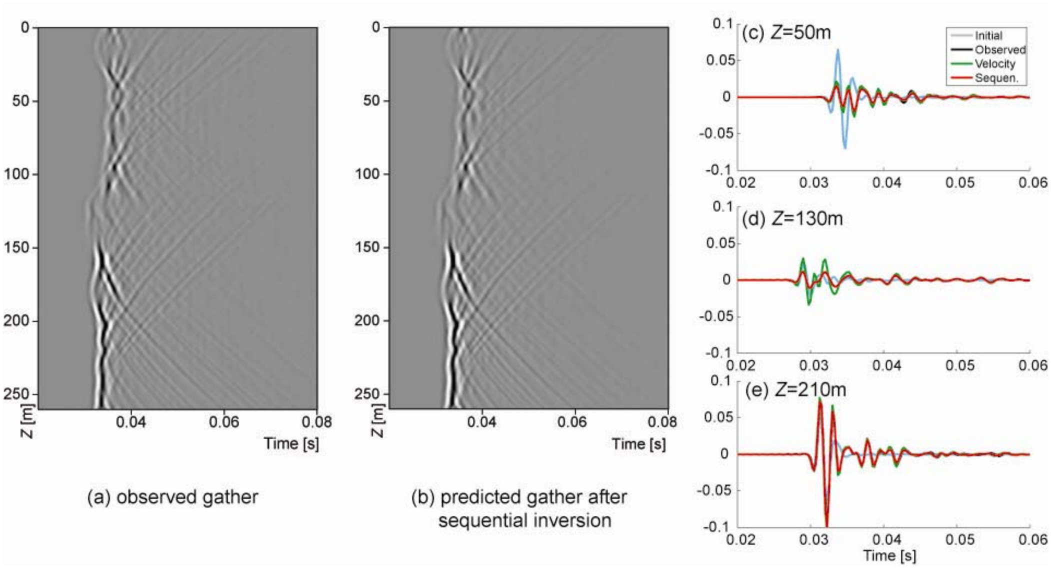

Figure 3: (a), (b) : Synthetic common level gathers using (a) true models and (b) predicted models from the sequential inversion. (c)-(e) : Comparison of simulated waveforms at (c) Z=50m (Layer 1) (d) Z=130m (Layer 2), and (e) Z=210m (Layer 3). Light blue lines indicate the waveforms simulated with the initial model, black lines with the observed model, green lines with the estimated model after the initial velocity inversion, red lines with the estimated model after the entire sequential inversion.

References

Hicks G. and Pratt R.G. [2001] Reflection waveform inversion using local descent methods: Estimating attenuation and velocity over a gas-sand deposit, *Geophysics*, **66**, 598-612

Kennett, B.L.N., Sambridge, M.S. Williamson, P.R. [1988] Subspace methods for large inverse problems with multiple parameter classes, *Geophysical Journal International*, **94**, 237-247

Liu, H.P., Anderson, D.L., Kanamori, H. [1976] Velocity dispersion due to anelasticity; implications for seismology and mantle composition , *Geophysical Journal of the Royal Astronomical Society*, **47**, 41-58

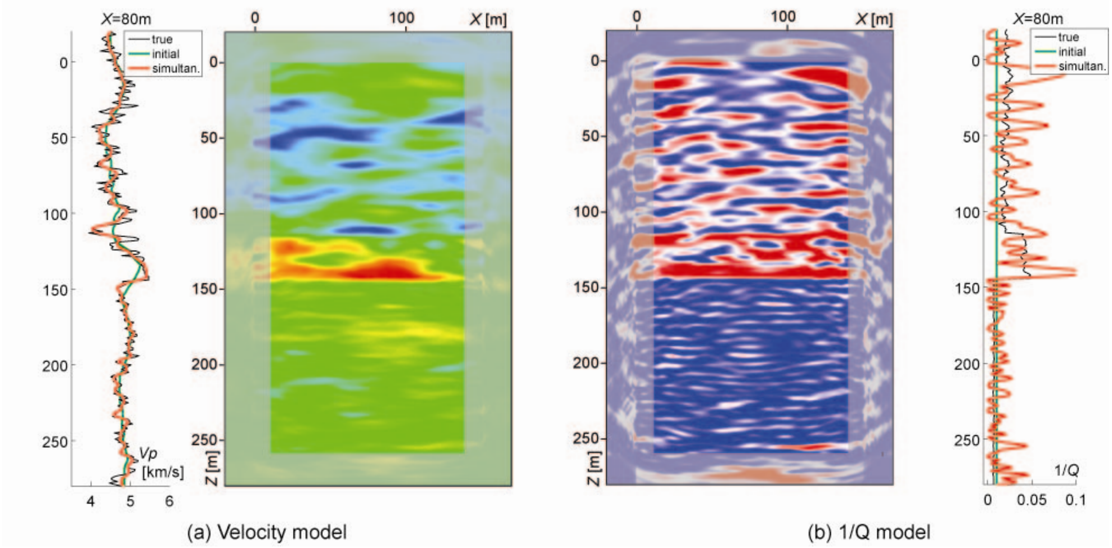

Figure 3: Inversion results from simultaneous inversion alone with their vertical profiles at X=80m. In the vertical profiles, black lines indicate the true models, green lines the initial models, and red lines the estimated models.

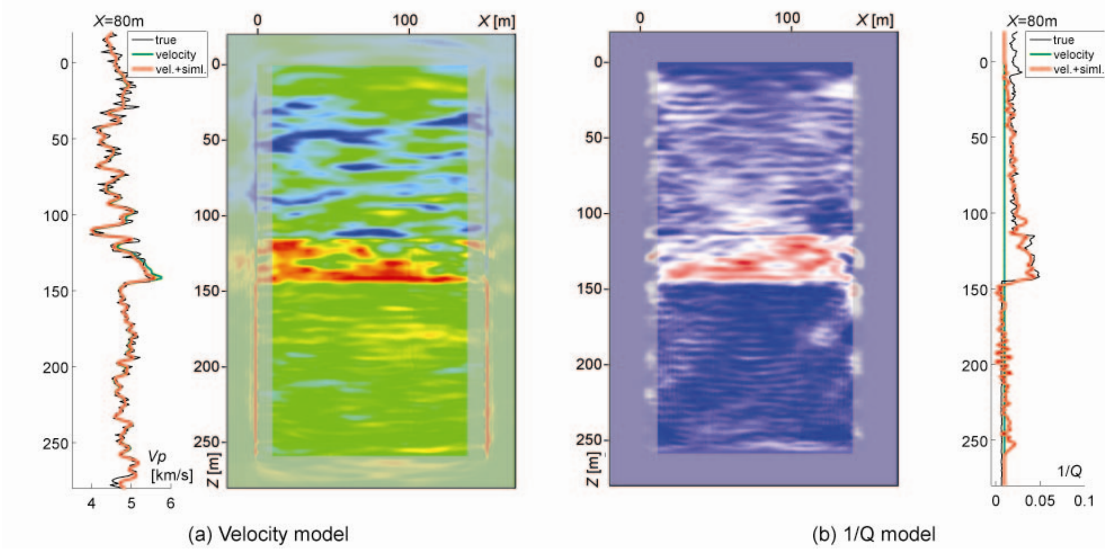

Figure 4: Inversion results from sequential inversion with their vertical profiles at X=80m. In the vertical profiles, black lines indicate the true models, estimated models after the initial velocity inversion, red lines the estimated models after entire sequential inversion.

Pratt, R.G., Hou, F., Bauer, K. and Weber, M.H. [2004] Waveform tomography images of velocity and inelastic attenuation from the Mallik 2002 Crosshole Seismic Surveys, in *Scientific results from the Mallik 2002 Gas Hydrate Production Research Well Program, Mackenzie Delta, North Territories, Canada, (ed.) S.R. Dallimore and T.S. Collet, Geological Survey of Canada, Bulletin*, **585**, 14p

Pratt, R.G., Shin C., Hicks, G. [1998] Gauss-Newton and full Newton methods in frequency-space seismic waveform inversion, *Geophysical Journal International*, **133**, 341-362,

Sirgue, L. [2003] Inversion de la forme d'onde dans le domaine frequential de donnees sismiques grands offsets. Ph.D. thesis, l'Ecole Normale Superieure de Paris.

Wu, R.S., and Toksoz, M.N. [1987], Diffraction tomography and multi-source holography applied to seismic imaging, *Geophysics*, **52**, 11-25